Mechanical, Thermal, and Biodegradation Studies of Polystyrene–Phthalated Starch Blends Using Epoxy Functionalized Compatibilizer

A. Ashamol, R. R. N. Sailaja

The Energy and Resources Institute, 4th Main, 2nd Cross, Domlur 2nd Stage, Bangalore, Karnataka 560071, India

Received 10 December 2009; accepted 20 July 2011
DOI 10.1002/app.35598
Published online 19 December 2011 in Wiley Online Library (wileyonlinelibrary.com).

ABSTRACT: Blends of polystyrene (PS) and esterified starch has been prepared using an epoxy functionalized PS as compatibilizer along with zinc stearate as prooxidant. The starch phthalate (Stph) loading was varied from 20 to 60%. The mechanical, thermal, and biodegradability studies of the blends were carried out as per the ASTM standards and the results were compared with that of neat PS. The blends exhibited enhanced mechanical properties with the addition of compatibilizer although the biodegradation rate slows down. The blend containing 40% starch ester with 12% compatibilizer showed maximum tensile strength. Thermogravimetric and differential scanning colorimetric analyses has been done for the blends, and the neat PS and the glass transition temperature of the blend has been obtained at 327 K. The water absorbency of the blends showed an increase with the increase in loading of Stph and a reduction with the addition of compatibilizer. © 2011 Wiley Periodicals, Inc. J Appl Polym Sci 125: 313–326, 2012

Key words: polystyrene; starch phthalate; compatibilizer; blends; biodegradation

INTRODUCTION

The consumption of petrochemical-based polyolefins is continuously on the rise owing to their light weight, flexibility, and easy processability. However, due to their increased consumption, there is a constant accumulation of nonbiodegradable plastic waste leading to disposal problems particularly for widely used polyolefins such as polyethylene, polystyrene (PS), etc. Thus, efforts to replace these plastics with inexpensive biopolymers such as starch, cellulose, etc., is being looked into. PS is widely used for protective food packaging and the post consumer packaging waste disposal is a problem. Thus, starch/synthetic polymer blends containing 70% starch was prepared by Ramaswamy and Bhattacharya.[1] Biodegradable binary blends of PS with degradable polymers such as polycaprolactone and poly(lactic acid) (PLA) were investigated.[2] It was found that PS/PLA composites exhibited better mechanical properties when compared with other fillers used. However, a blend of PS with a biopolymer is incompatible owing to their inherent structural differences. However, higher loadings of the biopolymeric materials would ensure degradability of the blend. Thus, surface modification via benzoylation of sisal fiber was carried out before blending with PS by Nair et.al.[3,4] The study of biodegradable films made from synthetic polymers such as low-density polyethylene with various types of starch has been done by Arvanitoyannis et al.[5–8] In all these studies, blends containing starch up to 30% showed better mechanical properties, and the biodegradability rate of the blends was enhanced when the starch content exceeded 10%.

The treated fibers were found to show better mechanical properties than composites made from untreated fibre/PS composites. It has been generally found that increased loading of the biopolymeric filler is detrimental to the mechanical properties. Thus, both surface treatment of filler and addition of compatibilizing agent help improve the mechanical properties close to unfilled or neat polymer. Thus, Mishra and Naik[9] blended PS with maleic anhydride treated banana, hemp, and sisal fibers leading to better fibre/matrix adhesion. Dynamic mechanical analysis of agricultural residues filled PS revealed an increase in dynamic modulus and viscosity.[10] Cassava starch grafted PS was synthesized by suspension polymerization technique by Kaewta and Varaporn,[11] thereby leading to nongelatinized starch-based materials. An in depth comprehensive review on the development of biodegradable polymers and their biodegradability has been analyzed by various researchers.[12–14] Composites of recycled

Correspondence to: R. R. N. Sailaja (sailajab@teri.res.in).
Contract grant sponsors: Department of Science and Technology (DST).

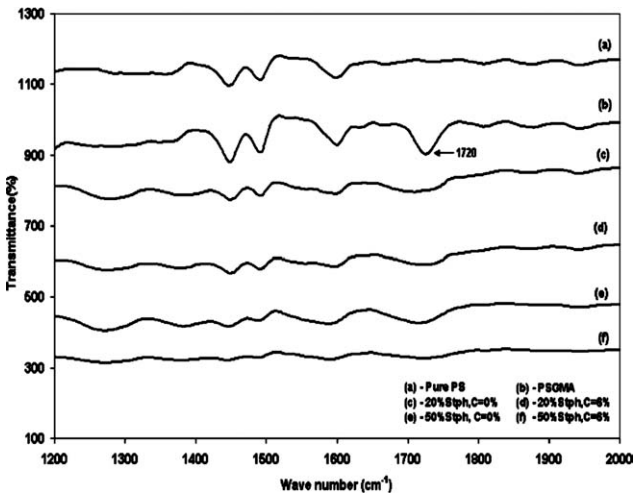

Figure 1 FTIR spectra of pure PS, PSGMA, and PS–Stph blends. (a) Pure PS, (b) PSGMA, (c) 20% Stph, C = 0%, (d) 20% Stph, C = 6% (e) 50% Stph, C = 0%, and (f) 50% Stph, C = 6%.

newspapers with PS showed improved modulus when compared with unfilled PS.[15] The effect of surface treatment of biopolymers from renewable resources and their contribution in enhancing filler/matrix adhesion was reviewed by Long et.al.[16] Blends of PS with thermoplastic starch using glycerol or buriti oil as plasticizer were examined for biodegradability by Daniela et al.[17] It was reported that the blends containing higher loadings of starch exhibited more biodegradability.

In this study, biodegradable blends of PS with Tapioca starch were prepared. Tapioca starch was modified by esterification using phthalic anhydride. Further, to enhance matrix filler adhesion, an epoxy functionalized PS was added as compatibilizer along with auto-oxidant additive. Compatibilizer is a polymeric interfacial agent that facilitates formation of uniform blends of normally immiscible polymers with desirable end properties. The blends were examined for mechanical, thermal, water uptake, and biodegradability characteristics.

MATERIALS AND METHODS

Materials

PS (GP525, Kerala, India) with melt flow index 1 g per 10 min was purchased from Saraswathi Plastics (Bangalore, India). Tapioca starch (14.2 μm) was obtained from the roots of tapioca plants grown in Kerala. Tapioca starch used in this study was purchased from Sugandha Kesari depot. Phthalic anhydride, zinc stearate, benzoyl peroxide (BPO), and common solvents were obtained from S.d. Fine Chem (Bangalore, India). Glycidyl methacrylate (GMA) monomer was obtained from Sigma Aldrich.

Preparation of Stph

Esterification of starch was done using phthalic anhydride. Starch (100 g) was added to 900 mL formamide and 10 g of potassium acetate. This solution was stirred for 1 h at 80°C. Phthalic anhydride (280 g) was then added and the reaction was continued for another 3 h at 80°C. This mixture was then poured into ice cold water for precipitation. Starch phthalate (Stph), which formed as precipitate, was washed several times with acetone for removing unreacted phthalic anhydride and then dried at room temperature.

Synthesis of compatibilizer

Polystyrene co-Glycidyl Methacrylate

The grafting of GMA to PS was done by reactive blending in a mini extruder (LME- 230 Dynisco). PS (46 g) is premixed with GMA/BPO, where the BPO content was 10–15% w/w of GMA content. The GMA content was 5–20% w/w of PS content. The mixture was then introduced into the chamber of the extruder having 40 cubic centimeter capacity. Mixing speed was kept at 60 rpm.

Characterization

Fourier transform infrared spectroscopy (FTIR) of pure PS, polystyrene *co*-glycidyl methacrylate (PSGMA), and the blends were carried out (Perkin–Elmer Spectrum 1000) and the respective spectra are shown in the Figure 1.

Preparation of blends

Different compositions of blends of PS–Stph with compatibilizer PSGMA were prepared according to the weight ratio 80 : 20, 70 : 30, 60 : 40, 50 : 50, and 40 : 60 (Table I). The amount of compatibilizer (PSGMA) added was based on the weight percent of starch ester, and the amount of pro-oxidant (zinc stearate) added was kept constant (0.1% of total weight). The blends were prepared by melt mixing at 120°C in a Brabender Plasticorder (CMEL, 16 CME SPL East Germany) and made into sheets by compression moulding (Hot Press Tester Labtech). The sheets were cut into rectangular strips and these strips were subjected to mechanical testing.

Mechanical properties of the blends

Tensile properties

The tensile properties of the blends and neat PS were measured by Zwick UTM (Zwick Roell, ZHU, 2.5) with Instron tensile flat surface grips at a cross head speed of 2 mm min^{-1}. The tensile tests were

TABLE I
List of Blend Compositions

Polystyrene		Starch phthalate		PSGMA	
Percentage	Grams	Percentage	Grams	Percentage	Grams
80	80.0	20	20.0	0	0.0
			19.4	3	0.6
			18.8	6	1.2
			18.2	9	1.8
			17.6	12	2.4
			17.0	15	3.0
70	70.0	30	30.0	0	0.0
			29.1	3	0.9
			28.2	6	1.8
			27.3	9	2.7
			26.4	12	3.6
			25.5	15	4.5
60	60.0	40	40.0	0	0.0
			38.8	3	1.2
			37.6	6	2.4
			36.4	9	3.6
			35.2	12	4.8
			34.0	15	6.0
50	50.0	50	50.0	0	0.0
			48.5	3	1.5
			47.0	6	3
			45.5	9	4.5
			44.0	12	6
			42.5	15	7.5
40	40.0	60	60.0	0	0.0
			58.2	3	1.8
			56.4	6	3.6
			54.6	9	5.4
			52.8	12	7.2
			51.0	15	9.0

performed as per ASTM D638 method. The specimens tested were of rectangular shape having length, width, and thickness of 7 cm, 1.5 cm, and 0.3 cm, respectively. A minimum of five specimens were tested for each variation in composition of the blend and results were averaged.

Flexural Properties

The flexural properties of the blends and pure PS were measured by Zwick UTM (Zwick Roell, ZHU, 2.5) with a preload speed of 10 mm min^{-1}. The tests were performed as per ASTM D 790-03 method. The samples were having a length of 5 cm, width of 2 cm, and a thickness of 0.3 cm. A minimum of four specimens were tested for each blend and the results were averaged.

Compressive Properties

The compressive properties of the PS–Stph blends and neat PS were measured by Zwick UTM (Zwick Roell, ZHU, 2.5) with a preload of 4.5 KN. The test speed was maintained at 2 mm min^{-1}. The tests were performed as per ASTM D 695. The samples were having a length of 3 cm, width of 2 cm, and a thickness of 0.3 cm. A minimum of four specimens were tested for each variation in composition and the results were averaged.

Thermal analysis of the blends

Thermogravimetric analysis

The thermogravimetric analysis (TGA) was carried out for the blends and for pure PS using Perkin–Elmer Pyris Diamond 6000 analyzer (Perkin–Elmer Inc, Shelten, (T)) in a nitrogen atmosphere. The sample was subjected to a heating rate of 10°C min^{-1} in a heating range of 40–600°C with Al_2O_3 as reference material.

Differential scanning colorimetry

Differential scanning colorimetry (DSC) of the blend specimen was carried out in a Mettler Toledo model DSC 822e instrument (Mettler Toledo AG, Switzerland). Samples were placed in the sealed aluminum cells with a quantity of less than 10 mg and scanning at a heating rate of 10°C min^{-1} in a heating range of 50–150°C in one run.

Blend morphology

Scanning electron microscopy (SEM; JEOL, JSM–840). A microscope was used to study the morphology of fractured and unfractured specimens. The specimens were gold sputtered (JEOL, SM-1100E) before microscopy. The SEM morphology of the unfractured specimens were determined after soaking the blend specimens in 5% v/v sulphuric acid for 24 h and then washed thoroughly and dried in air.

Biodegradation

The biodegradation of the blend specimens and the pure PS was carried out by soil burial method as per ASTM D5338-98. Soil-based compost was taken in small chambers. Humidity of the chambers was maintained at 40–45% by sprinkling water. The chamber were stored at 30–35°C. Rectangular specimens were buried completely into the wet soil at a depth of 10 cm. Samples were removed from the soil at constant time intervals (15 days) and washed gently with distilled water and dried in vacuum oven at 50°C to constant weight. Weight loss percentage of the samples with respect to time was recorded as a measure of biodegradation.

Water absorption

Water absorption of the blend specimen and for pure PS was carried out as per ASTM D570-81. This test of dried specimens was evaluated according to

mass changes of the samples after their immersion in distilled water for 24 h under ambient conditions. The size of the samples was 10 × 10 mm^2. The weight gain percentage of the samples was recorded as a measure of water absorption.

RESULTS AND DISCUSSION

Biodegradable blends of PS with esterified starch were made using an epoxy functionalized compatibilizer. The mechanical, thermal, water uptake, and biodegradability studies of these blends have been carried out.

FTIR spectroscopy

Figure 1 shows the FTIR spectra of grafted PSGMA and that of the blends. Pure PS is also shown in the figure [curve (a)] for the sake of comparison. The grafted PS, that is, PSGMA [curve (b)], exhibits a characteristic peak for carbonyl group, which is observed at 1720 cm^{-1}. The compatibilized blends with 20% [curve (c)] and 50% [curve (d)] Stph loading does not have this characteristic peak indicating that reactive blending has taken place.

Effect of compatibilizer

Figure 2(a–c) shows the effect of compatibilizer on the mechanical properties of PS–Stph blends. Figure 2(a) shows the effect of percentage compatibilizer on the relative tensile strength (RTS; i.e., tensile strength of blend/tensile strength of neat PS). For 20% Stph loading, the RTS value drops down to 70% of that of neat PS. Compatibilized blends exhibit RTS value close to that neat PS. For higher loadings of 30–50% Stph, the RTS values of compatibilized blends is greater than 0.85. For 60% Stph loading, the RTS value is around 70% of that of neat PS. The epoxy group of the compatibilizer undergoes chain scission and reacts with the ester and unreacted hydroxyl groups of esterified starch. The possible reaction mechanism is shown in Figure 3. This facilitates in anchoring the starch derivative with PS. This improves the dispersion of Stph in PS, which in turn enhances the tensile strength values. Figure 2(b) shows the effect of compatibilizer on relative tensile modulus (relative Young's modulus; RYM) values of PS–Stph blends. The modulus values of PS–Stph blends are close to that of neat PS. For higher loadings of 50 and 60% Stph, the RYM values slightly reduce to ~0.9 due to the mild plasticizing effect of Stph. It has been earlier observed by Sagar and Merrill[18] that the ester groups act as an internal plasticizer. However, compatibilization brings the RYM values close to that of neat PS. Figure 2(c) shows the plot of relative elongation at break (REB) versus percentage compatibilizer for PS–Stph blends. The REB values decreases as Stph loading increases. For 20 and 30% Stph loading, compatibilization increases the REB values to around 77% of that of neat PS. For higher loadings of 40 and 50%, the elongation at break values is approximately 70% for compatibilized

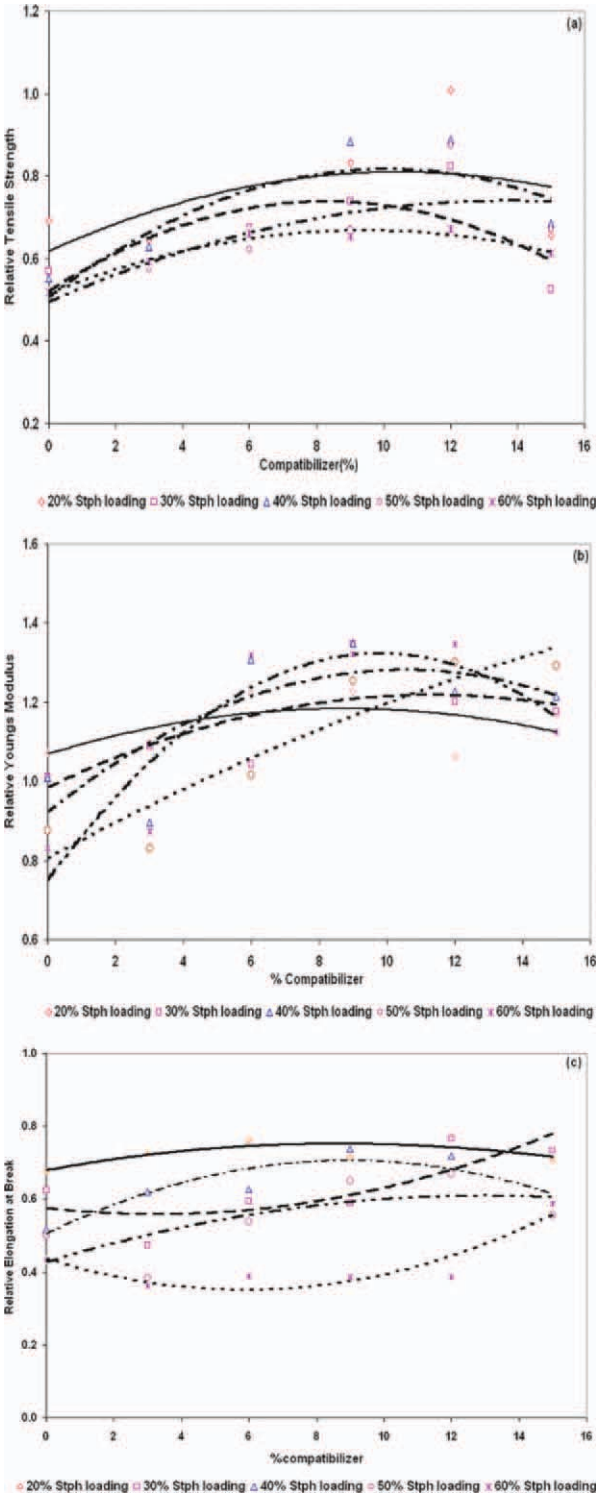

Figure 2 Possible reaction mechanism between PSGMA and Stph. [Color figure can be viewed in the online issue, which is available at wileyonlinelibrary.com.]

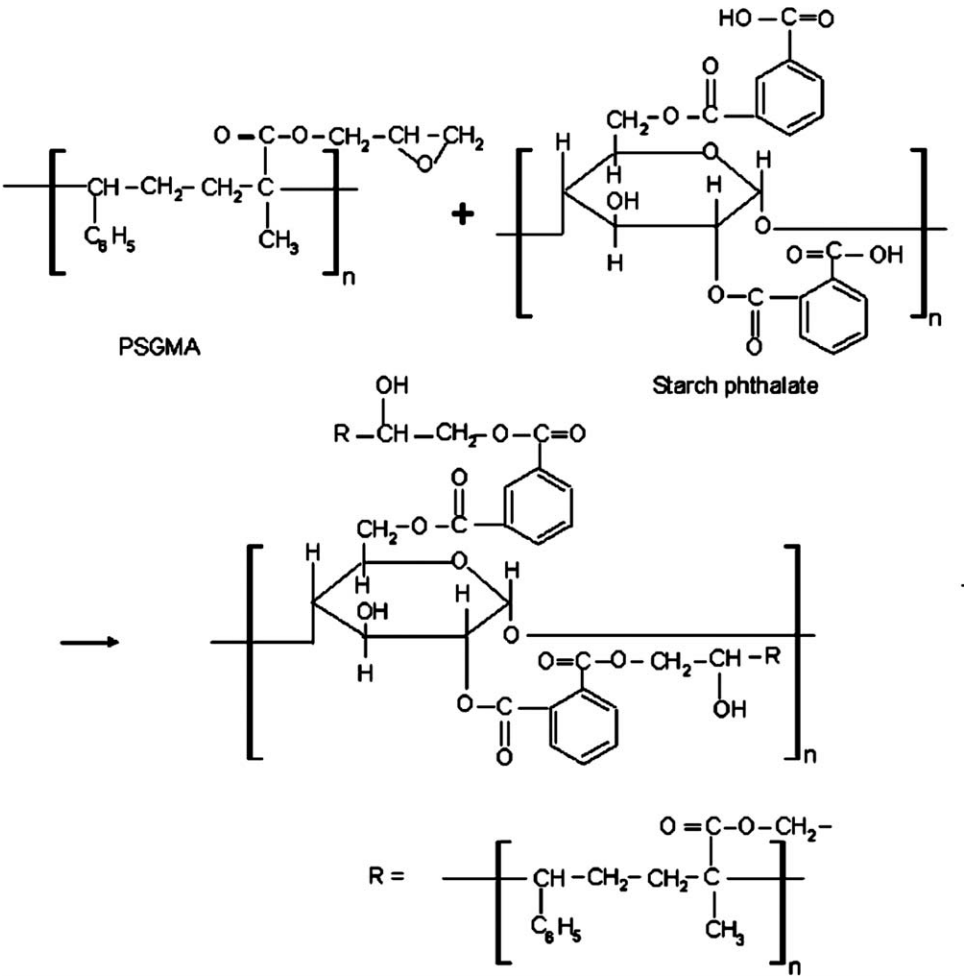

Figure 3 Plots of relative tensile properties versus percentage compatibilizer. (a) RTS, (b) RYM, and (c) REB.

blends owing to improved adhesion. All blends exhibit an optimal compatibilizer content of 12% beyond which compatibilization is detrimental to the mechanical properties of the blend.

Effect of Stph loading RTS

The Figure 4(a–f) shows the plots of volume fraction of Stph on RTS (relative to neat PS) values for PS–Stph blends. As the Stph loading increases, the RTS values reduce to around 0.52 for 60% Stph loading [Fig. 4(a)]. Compatibilization improves RTS values closer to neat PS due to reactive blending between PSGMA and Stph. For 20% Stph loading, the RTS value is very close to that of neat PS on compatibilization. For 30% Stph loading, the RTS value increases from 0.57 to 0.83 on adding compatibilizer. For higher, that is, 40 and 50% Stph loading, tensile strength values increase from 55% (no compatibilizer) to 89% and 88% (with compatibilizer of that of neat PS, respectively). For still higher loading of 60% Stph, the blends registered a 30% increase in tensile strength values. Two theoretical models have been used to further analyze the obtained experimental results. The volume fraction of Stph (ϕ) has been calculated from the weight fraction using the following eq. (1).

$$\phi_i = \frac{(w_i/\rho_i)}{\Sigma(w_i/\rho_i)} \tag{1}$$

In eq. (1), w_i and ρ_i are the weight fraction and density, respectively, of component i in the blend. The density values of PS, Stph, and PSGMA are, respectively, 1.05, 0.752, and 1.16.

The first model is the Halpin–Tsai model,[19] which is given below in eq. (2).

$$\text{RTS} = \frac{\sigma_b}{\sigma_o} = \frac{1 + G\eta_T\phi}{1 - \eta_T\phi} \tag{2}$$

In eq. (2), the variable η_T is given by the following equation,

$$\eta_T = \frac{R_T - 1}{R_T + G} \tag{3}$$

In eq. (3), R_T is the ratio of filler tensile strength to the tensile strength of neat PS.

The constant G is given by eq. (4) as follows:

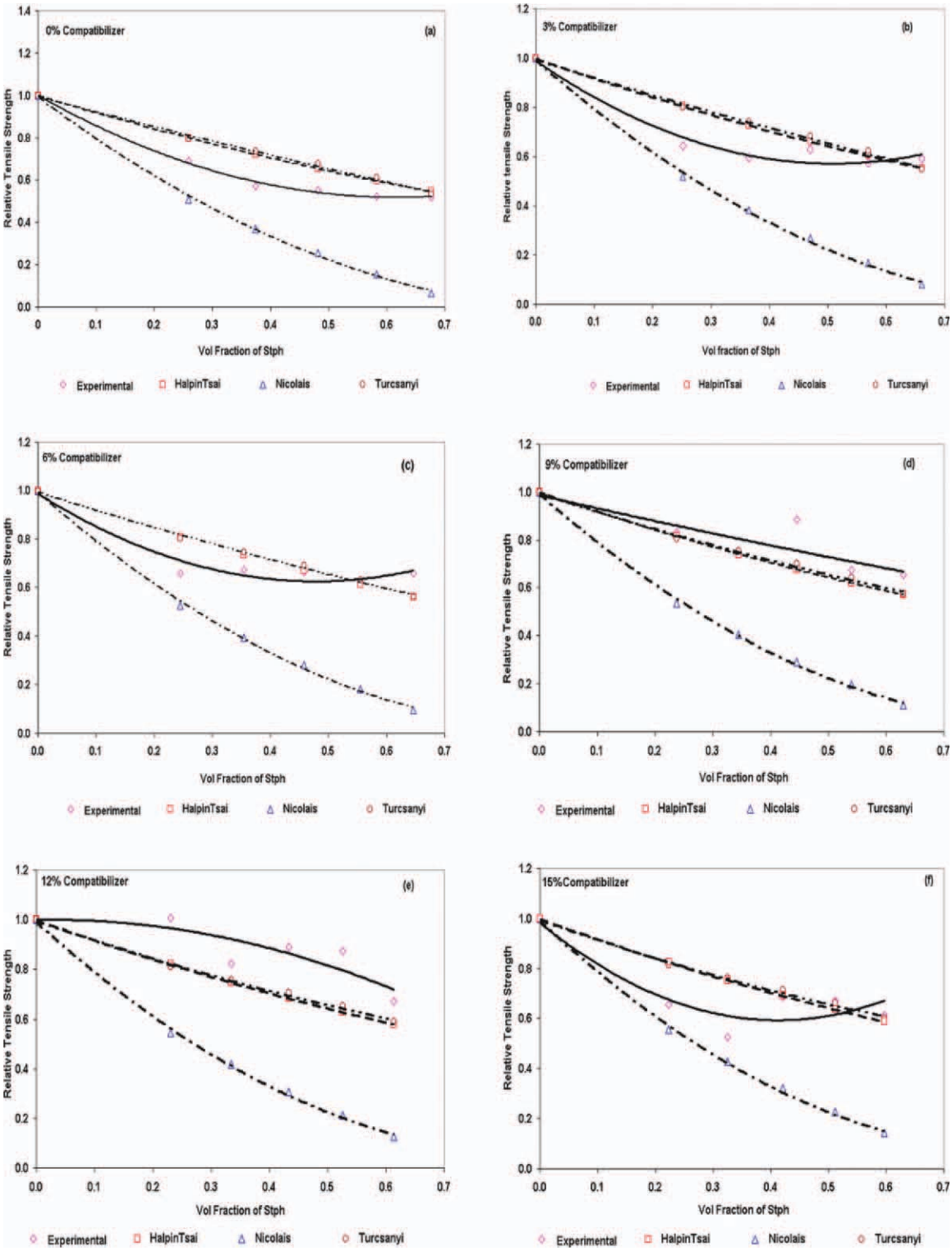

Figure 4 Variation of RTS with volume fraction of Stph. 0% compatibilizer, (b) 3% compatibilizer, (c) 6% compatibilizer, (d) 9% compatibilizerc, (e) 12% compatibilizer, and (f) 15% compatibilizer. [Color figure can be viewed in the online issue, which is available at wileyonlinelibrary.com.]

$$G = \frac{7 - 5\upsilon}{8 - 10\upsilon} \tag{4}$$

Where, υ is the Poisson's ratio of PS taken to be 0.33.[20] R_T was calculated to match with the experimental results and this was found to be 0.07. The theoretical values obtained from eq. (3) are shown in Figure 4. Figure 4(a) for 0% compatibilizer shows that the experimental values are lower than those predicted by Halpin–Tsai model that assumes good

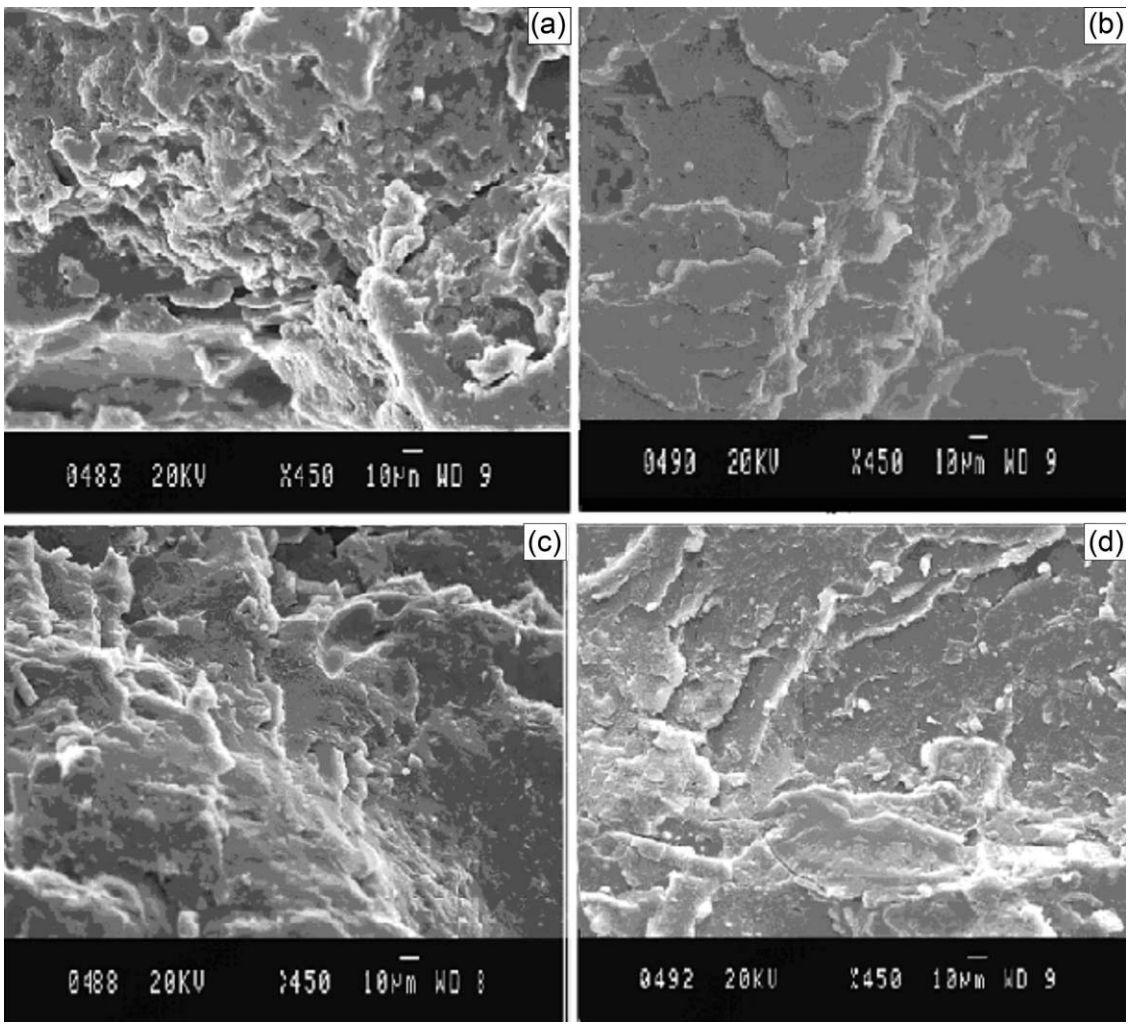

Figure 5 Scanning electron micrographs showing tensile fracture surfaces for the blends. (a) 20% Stph, C = 0%, (b) 20% Stph, C = 12%, (c) 40% Stph, C = 0%, and (d) 40% Stph, C = 12%.

adhesion. For 3 and 6% compatibilizer [Fig. 4(b,c)], the experimental values are lower than those calculated using eq. (2). However, Figure 4(d,e) shows better agreement with the Halpin–Tsai model owing to improved dispersion and bonding between filler and matrix.

The second model includes a parameter B for interfacial adhesion and is described by Turcsanyi model as[20] follows:

$$\mathrm{RTS} = \frac{\sigma_b}{\sigma_o} = \frac{1-\phi}{1+2.5\phi}\exp(B\phi) \qquad (5)$$

In the above equation, B was found to be 2.2, which indicates good matrix–filler adhesion. A similar observation has been made by Zou et.al.[21] for three different fillers in a biodegradable aliphatic polyester. It was reported the filler–matrix combination with the maximum B value was found to exhibit better tensile strength when compared with other filler–matrix combinations for no adhesion, (B is 0.25).However, as the filler–matrix adhesion improves, the value of B increases. Thus, in this study, the obtained B value (2.2) indicates good adhesion as observed in Figure 4.

In Figure 4(a), the obtained experimental values are lower than the predicted values owing to the incompatibility between polar Stph and non polar PS. However, in Figure 4(b–e), (compatibilized blends), the experimental RTS values move closer to the predicted values. The theoretical values of the Halpin–Tsai and Turcsanyi model are close to each other as observed in Figure 4(b–e). Thus, the experimental values suggest improved adhesion could be achieved even for high loadings of the starch derivative. However, in Figure 4(f), the theoretical values do not match owing to the presence of excessive compatibilizer.

The morphology of tensile fracture surfaces are shown in Figure 5. Figure 5(a) shows fractured sample with 20% Stph loading (uncompatibilized) and is typical of brittle fracture with debonded Stph particles. The compatibilized counterpart in Figure 5(b) exhibits a similar morphology, although the dispersed particles

size is lower due to better interfacial adhesion. For 40% Stph loading [Fig. 5(c)], the micrograph shows large holes left by the cavitation of agglomerated Stph particles. The compatibilized blend [Fig. 5(d)] shows brittle fracture but the small deformed voids left by the debonded Stph particles can be seen throughout the entire area of the fractured surface. This indicates that the Stph particles are finely dispersed in the blend due to the addition of compatibilizer.

This is also reflected as high tensile strength values for the compatibilized blends. A similar observation for compatibilized PS blends was reported by Zheng et.al.[22] It was argued that the mode of energy absorption is mainly attributed to crack bifurcation or crack path alternation. This enables efficient stress transfer from matrix to filler

Relative Young's modulus

Figure 6(a–f) shows the plots of effect of Stph volume fraction versus RYM (relative to neat PS). The RYM values slightly increase with increase in filler loading upto 40%. For Stph loadings beyond 40%, the RYM values reduce owing to the plasticizing effect of the ester group [Fig. 6(a)]. A similar effect on RYM values was reported for glycerol plasticized starch thermoplastic starch (TS)—low density polyethylene (LDPE) blends in which case, the RYM values decreased with increase in TS loading[23] due to the plasticizing effect of glycerol. Compatibilization improves the RYM, close to that of neat PS as observed in Figure 6(b–f). Three theoretical models have been used to further analyze the obtained experimental results. The first is the Kerner's model[19] which considers no interaction between filler and matrix and is given below as follows:

$$\mathrm{RYM} = \frac{E_b}{E_{\mathrm{PS}}} = 1 + \left(\frac{\phi}{1-\phi}\right)\left(\frac{15(1-\upsilon)}{(8-10\upsilon)}\right) \tag{6}$$

The values determined using eq. (6) are also plotted in Figure 6. The predicted values do not match with the experimental values. For better matrix filler interactions, the Halpin–Tsai[19] model is given as following eq. (7) below.

$$\mathrm{RYM} = \frac{1 + G\eta_m\phi}{1 - \eta_m\phi} \tag{7}$$

where, the variable η_m is given by the following equation.

$$\eta_m = \frac{R_m - 1}{R_m + G} \tag{8}$$

In eq. (8), R_m is the ratio of filler modulus to matrix modulus. The R_m value was determined by trial and error to match with the experimentally observed values and has been found to be 1.65. For the uncompatibilized blends, the predicted values from eq. (7) deviates as the volume fraction of Stph increases.

However, for compatibilized blends, Figure 6(c–f), the theoretical values match closely with the obtained experimental values owing to better load transfer from matrix to filler and improved interface linking, thereby, enhancing the modulus values close to that of neat PS. The third model includes adhesion parameters for the two extreme conditions. For poor matrix–filler adhesion, the matrix pulls away from the filler surface and ξ value is equal to 1.0, while for perfect adhesion, $\xi = 0$.[21] The equation for this Sato-Furukawa model is given below in eq. (9).

$$\mathrm{RYM} = \frac{E_\sigma}{E_{\mathrm{PS}}} = \left[\left((1 + \frac{\phi^{2/3}}{2 - 2\phi^{1/3}}\right)(1 - \psi\xi) - \frac{\phi^{2/3}\psi\xi}{\left(1 - \phi^{1/3}\right)\phi}\right] \tag{9}$$

where,

$$\psi = \left(\frac{\phi}{3}\right)\left(\frac{1 + \phi^{1/3} - \phi^{2/3}}{1 - \phi^{1/3} + \phi^{2/3}}\right) \tag{10}$$

The value of ξ was found to be 0.8, which indicates that the matrix–filler adhesion is between the two extremes as shown in Figure 7.

Relative elongation at break

Figure 7(a–f) shows the REB (relative to neat PS) values versus volume fraction of Stph. The REB values reduce as Stph loading increases from 20 to 60%. The epoxy functionalized compatibilizer improves the REB values closer to that of neat PS. The experimental values obtained were analyzed using Nielsen model for perfect adhesion[24] given below.

$$\mathrm{REB} = \frac{\epsilon_b}{\epsilon_{\mathrm{PS}}} = \left(1 - 1.K\phi^{1/3}\right) \tag{11}$$

In eq. (11), ϵ_b and ϵ_{PS} are the elongation at break values for the blend and pure PS, respectively.

The adjustable parameter K in eq. (11) depends on filler geometry. The parameter K was varied so as to match with the experimental results and has been found to be 0.65. The theoretical values obtained from eq. (11) are also plotted in Figure 8. The experimental values do not match with the predicted values owing to poor adhesion for uncompatibilized blends [Fig. 7(a)]. As the compatibilizer content increases, the predicted values and experimental values [Fig. 7(c–f)] come closer. For Stph loading up to

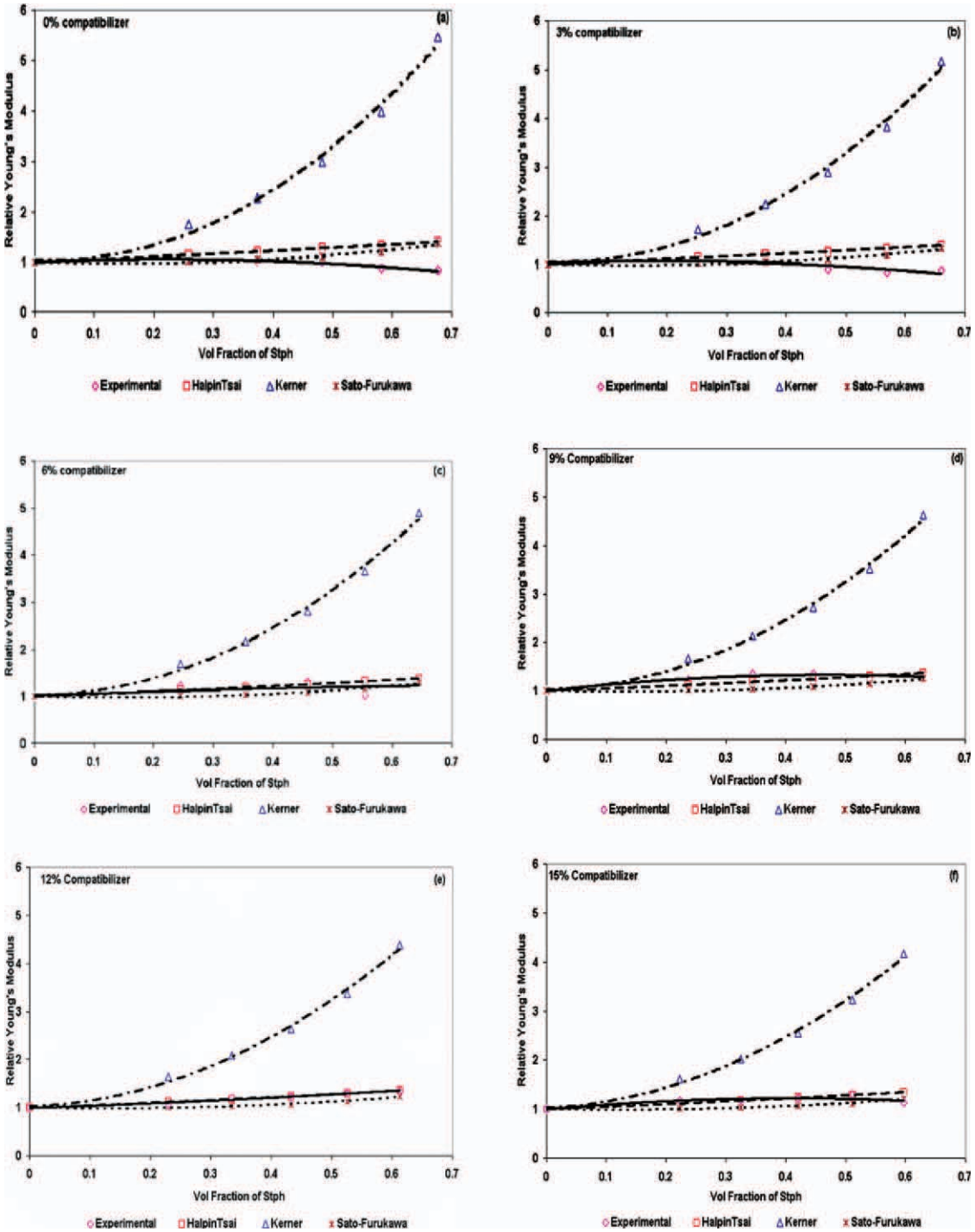

Figure 6 Variation of RYM versus volume fraction of Stph. (a) 0% compatibilizer, (b) 3% compatibilizer, (c) 6% compatibilizer, (d) 9% compatibilizer, (e) 12% compatibilizer, and (f) 15% compatibilizer. [Color figure can be viewed in the online issue, which is available at wileyonlinelibrary.com.]

40%, the compatibilized blends exhibit REB value of 0.72, that is, 72% of neat PS. For higher loading, that is, 50%, the REB value is 0.67. For 60% Stph loading, the elongation at break is 59% of that of neat PS as observed in 7(f). This improvement in REB values may be attributed to efficient anchoring by the epoxy functionalized compatibilizer. Furthermore, the ester group of PSGMA also blends effectively with esterified starch.

Relative compressive strength (RCS)

Table II shows the relative compressive strength (RCS, i.e., relative to neat PS) values for PS–Stph

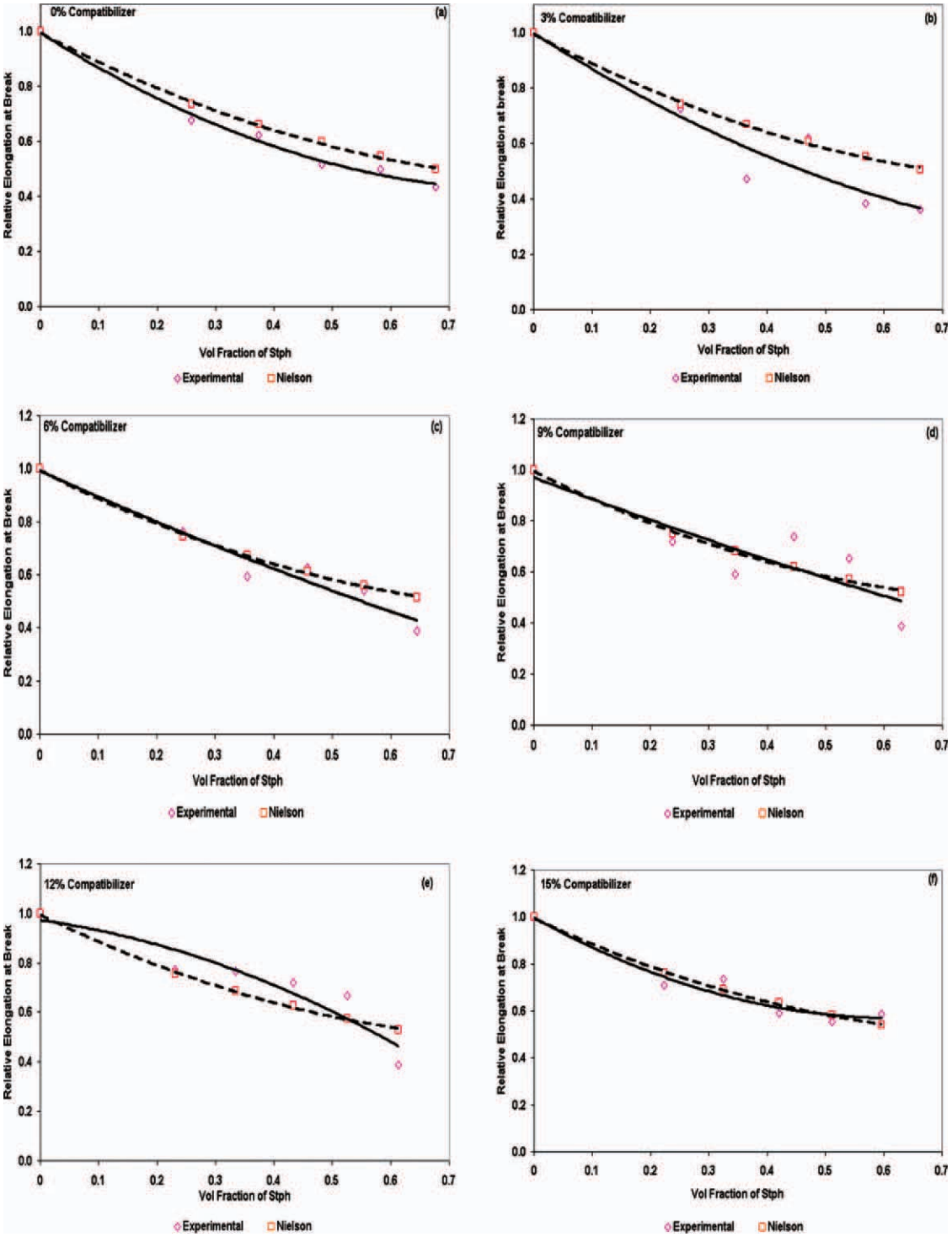

Figure 7 Variation of REB versus volume fraction of Stph. (a) 0% compatibilizer, (b) 3% compatibilizer, (c) 6% compatibilizer, (d) 9% compatibilizer, (e) 12% compatibilizer, and (f) 15% compatibilizer. [Color figure can be viewed in the online issue, which is available at wileyonlinelibrary.com.]

blends. The RCS values do not change considerably up to 40% Stph. However, for still higher loading of Stph, that is, 50 and 60%, there is a sharp fall in RCS values. Compatibilization improves RCS values to approximately 80% of that of neat PS for 20–40% Stph loading. For 50% Stph loading, the RCS value increases from 0.57 to 0.71 on adding compatibilizer. For 60% Stph loading, the RCS value increases by 23% and is 65.4% of that of neat PS.

Relative compressive modulus

Table II shows the relative compressive modulus (RCM; relative to neat PS) values for PS–Stph

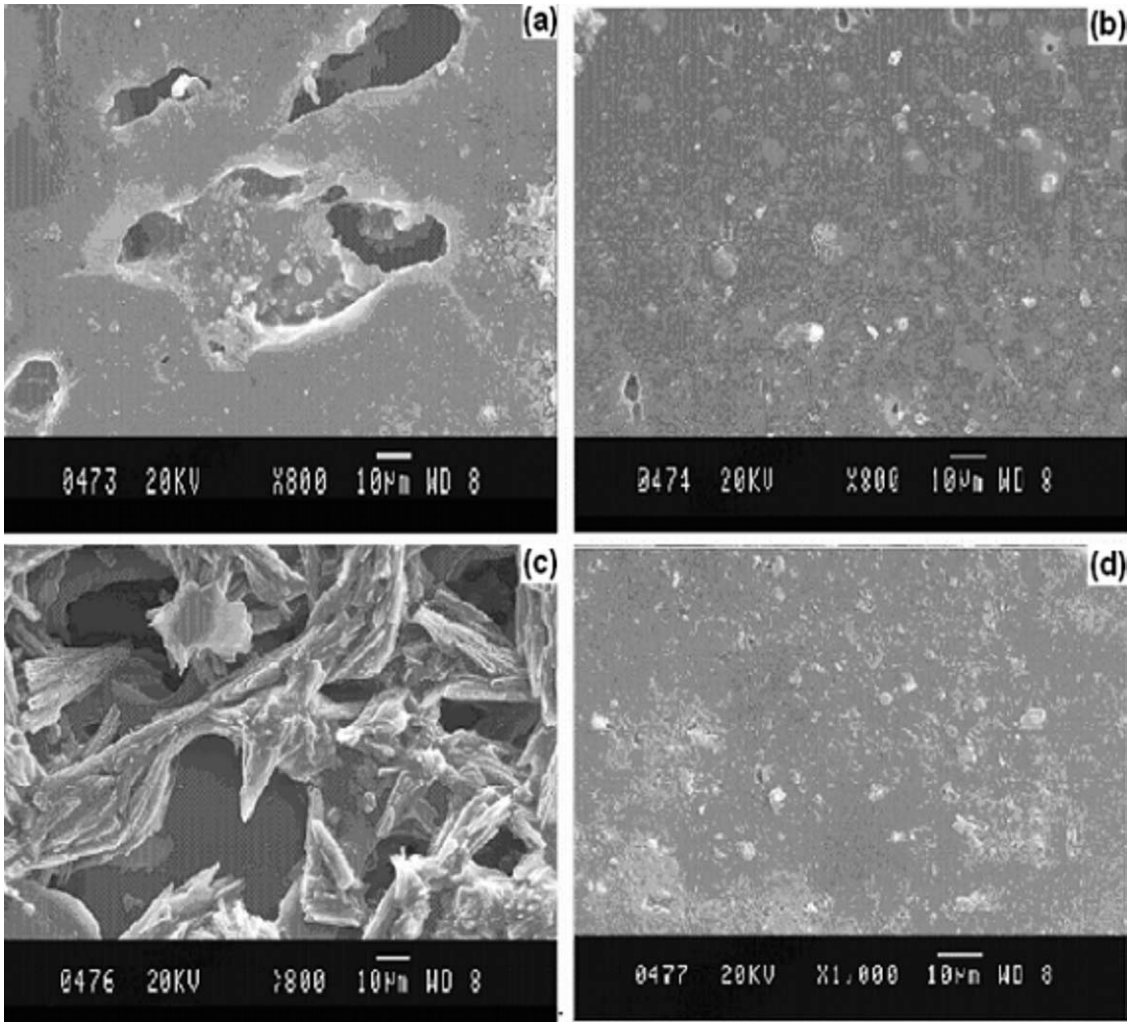

Figure 8 Scanning electron micrographs showing morphology of PS–Stph blend specimens. (a) 40% Stph, C = 0%, (b) 40% Stph, C = 6% (c) 60% Stph, C = 0%, and (d) 60% Stph, C = 6%.

blends. The RCM values increase as Stph loading increases from 20 to 60%, but they are lower than neat PS. Addition of compatibilizer for 20 and 30% Stph loading increases the RCM values to 0.78 and 0.79, respectively. For 40 to 60% Stph loading, compressive modulus is at par with neat PS. This considerable improvement in modulus values even for such high loading of Stph indicates improves good interaction between the matrix and filler due to the reaction of the epoxy functionalized compatibilizer with the blend components. Thus, this also leads to better stress transfer from matrix to filler causing resistance to compressive failure.

TABLE II
RCS and RCM Value of Polystyrene–Starch Phthalate Blends

%C	20% Stph	30% Stph	40% Stph	50% Stph	60% Stph
Relative compression strength values [RCS]					
0	0.65	0.66	0.68	0.56	0.53
3	0.67	0.69	0.71	0.59	0.46
6	0.70	0.73	0.75	0.66	0.59
9	0.71	0.74	0.77	0.69	0.62
12	0.75	0.80	0.81	0.71	0.65
15	0.62	0.48	0.77	0.69	0.62
Relative compression modulus values [RCM]					
0	0.63	0.63	0.74	0.76	0.65
3	0.63	0.63	0.78	0.89	0.68
6	0.64	0.65	0.79	0.90	0.70
9	0.71	0.73	0.94	1.00	0.76
12	0.78	0.791	1.03	1.05	0.98
15	0.72	0.76	0.87	1.01	0.759

Relative flexural strength

Table III shows the relative flexural strength (RFS; relative to neat PS) values for PS–Stph blends. The flexural strength for all uncompatibilized blends is lower than that of neat PS. However, compatibilization improves the RFS values owing to improved matrix–filler bonding. In all blends, optimal compatibilizer content is observed. Further addition of compatibilizer is detrimental to the flexural strength of

TABLE III
RFS and RFM Value of Polystyrene–Starch Phthalate Blends

%C	20% Stph	30% Stph	40% Stph	50% Stph	60% Stph
RFS values					
0	0.64	0.59	0.44	0.47	0.42
3	0.74	0.42	0.47	0.58	0.31
6	1.20	0.45	0.47	0.31	0.46
9	1.31	1.03	0.51	1.06	0.57
12	0.59	0.59	0.54	0.62	0.45
15	0.511	0.29	0.49	0.53	0.41
RFM values					
0	0.79	0.95	0.96	1.03	1.08
3	0.84	0.98	1.03	1.13	1.29
6	0.86	1.07	1.075	1.39	1.44
9	0.88	1.17	1.21	1.44	1.33
12	0.93	1.31	1.44	1.52	1.50
15	0.67	1.24	1.17	1.42	1.38

the blends. For 20 and 30%, the RFS values reach a maximum of 1.31 and 1.03, respectively. For 40%, the flexural strength is close to that of neat PS. For loadings of 50 and 60%, the RFS values are 1.06 and 0.57, respectively, owing to effective stress transfer between the two phases even at such high loadings.

Relative flexural modulus

Table III shows the relative flexural modulus (RFM; relative to neat PS) values for PS–Stph blends. For 20% Stph loading, the flexural modulus reduces. However, with the addition of compatibilizer, flexural modulus increases to 93% of that of neat PS. For 30 and 40% Stph loading, the compatibilized blends exhibit higher flexural modulus at par with neat PS owing to better interfacial adhesion between PS and Stph. For higher loadings of 50 and 60% loading, the blends, exhibit a slightly higher RFM values than neat PS.

Blend morphology

Figure 8(a–d) shows the blend morphology of PS–Stph blends loaded with 40 and 60% Stph. Figure 8(a) shows the blend morphology of PS–Stph containing 40% Stph without compatibilizer. The SEM micrograph shows large holes formed by the removal of agglomerated Stph. As PS and Stph are not compatible, Stph particles tend to coagulate in the blend. The compatibilized counterpart [Fig. 8(b)] shows a smooth surface with smaller elongated voids indicating finer dispersion of Stph in the PS matrix. This effect of agglomerated Stph particles in more pronounced for still higher loading of 60% Stph [Fig. 8(c)]. The compatibilized blend [Fig. 8(d)] shows a smooth surface with a number of elongated voids everywhere on the surface owing to better dispersion and bonding between filler and matrix thereby, giving resistance for the removal of Stph particles.

Thermogravimetric analysis

Figure 9 shows the TGA thermograms for neat PS and PS–Stph blends. Pure PS shows a single peak at 670.6 K with 80% weight loss [curve (a)] due to the breakage of —C—C— chains. Pure starch [curve (b)] also shows a single degradation peak at 580 K due to the ring scission of glucosidic units.[25] Stph [curve (c)] shows lower stability than unmodified starch due to the plasticizing effect of the phthalate group. A two stage degradation at 462 K and 546 K is observed for Stph. The uncompatibilized blend with 40% Stph [curve (d)] shows a two stage degradation at 528.6 and 608.2 K for the degradation of Stph and PS, respectively. The compatibilized blend with 40% Stph [curve (e)] also shows a similar two stage degradation at 528.6 and 608.2 K for the degradation of Stph and PS respectively. The compatibilized blend with 40% Stph [curve (e)] also shows a similar trend as [curve (d)] except that the weight loss is higher (70.5%) when compared with the uncompatibilized blend (57.3% at loss) at 608.2 K.

TGA analysis is important from the viewpoint of quality control and processing temperature for the blends.

DSC thermograms

DSC thermograms of the blends are shown in Figure 10. The DSC thermograms of pure PS and Stph are also shown in the figure for the sake of comparison. The T_g value of pure PS has been found to be at 368.5 K which matches with the value obtained by

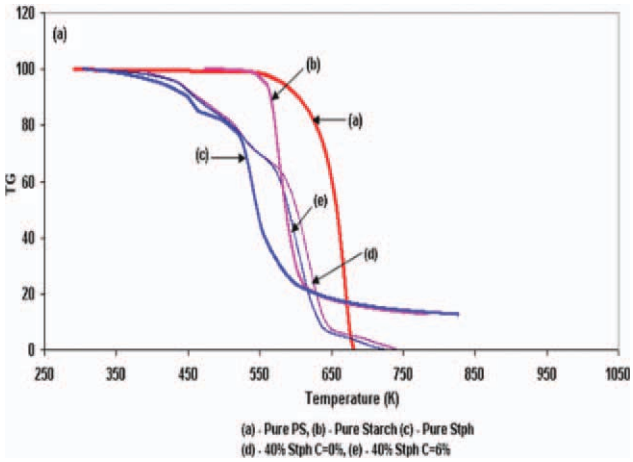

Figure 9 TG thermograms for pure PS, starch, Stph, and PS–Stph blends. (a) Pure PS, (b) pure starch, (c) pure Stph, (d) 40% Stph, C = 0%, (e) 40% Stph, C = 6%, (f) 60% Stph, C = 0%, and (g) 60% Stph, C = 6%. [Color figure can be viewed in the online issue, which is available at wileyonlinelibrary.com.]

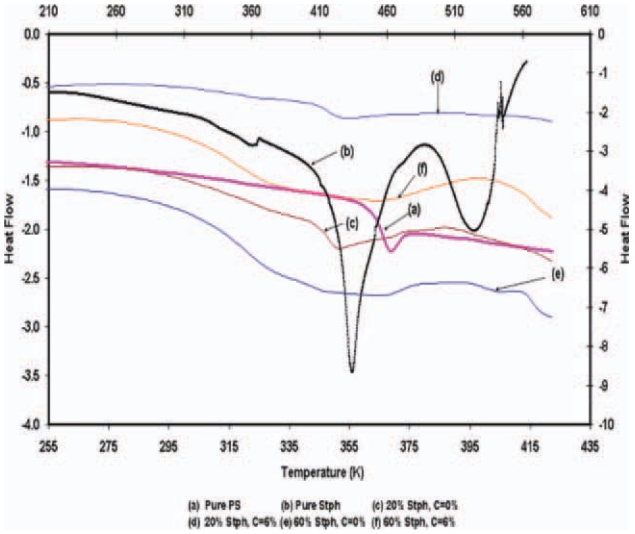

Figure 10 DSC thermograms for pure PS, pure Stph, and PS–Stph blends. (a) Pure PS, (b) pure Stph, (c) 20% Stph, C = 0%, (d) 20% Stph, C = 6%, (e) 40% Stph, C = 0%, (f) 40% Stph, C = 6%, (g) 50% Stph, C = 0%, (h) 50% Stph, C = 6% (i) 60% Stph, C = 0%, and (j) 60% Stph, C = 6%. [Color figure can be viewed in the online issue, which is available at wileyonlinelibrary.com.]

Nassar et.al.[26] The T_g value for pure stph is at 434.5 K. Similar observation for starch ester has been reported by Yang and Montgomery (which is 429 K).[27] The T_g value for the blends is given in Table III. The T_g values for the blends are lower than either of the components. As stph loading increases from 20 to 60%, there is a depression in T_g value from 350.5 K (for 20% stph) to 323.5 K (for 60% stph). This depression may be due to presence of ester linkages, which function as internal plasticizer as mentioned earlier.

Water uptake

Table IV shows the variation of percentage water absorption with Stph loading. The water absorption for the blends increase with increase in Stph loading for both compatibilized and uncompatibilized blends. However, the compatibilized blends show lower water absorption than their uncompatibilized counterparts.

TABLE IV
Water Absorption Analysis of Polystyrene–Starch Phthalate Blends

	Water uptake (%)		
Stph loading (%)	0% C	9% C	Standard deviation
20	4.25	2.14	1.49
30	15.01	12.48	1.79
40	21.2	8.83	8.75
50	17.69	9.25	5.97
60	45.56	23.76	15.41

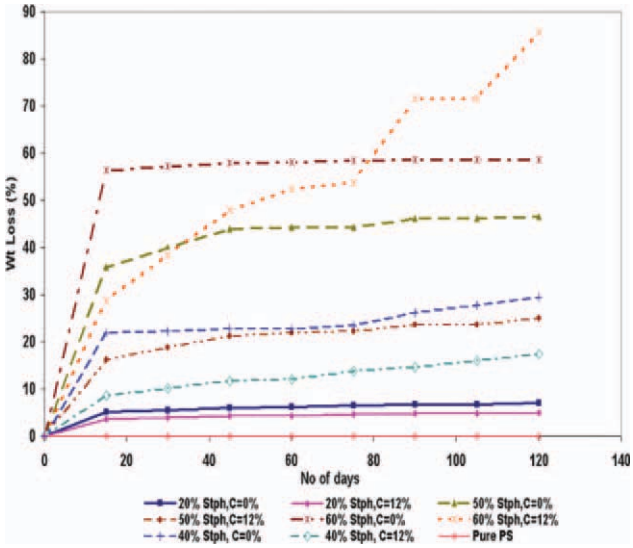

Figure 11 Biodegradation: variation of percentage weight loss with number of days for PS–Stph blends and for pure PS. [Color figure can be viewed in the online issue, which is available at wileyonlinelibrary.com.]

Untreated starch absorbs a large amount of water but replacement of these hydrophilic hydroxyl groups by ester groups lowers the absorbed water content.[28,29] Thus, the reduction in water uptake on compatibilization may be attributed to the formation of covalent bonds of Stph with the PSGMA compatibilizer.

Biodegradation

Figure 11 shows the percentage weight loss of PS–Stph blends with time. The biodegradability increased as Stph content increased from 20 to 60%. For 20–50% Stph loading, compatibilized blends exhibited lower biodegradability rates than uncompatibilized blends. A similar observation was reported by Tserki et.al.[29] Hydrophilicity facilitates biodegradation and esterification using phthalic anhydride partially substitutes the hydroxyl groups and hence biodegradation rates and lowered. As compatibilization further enhances the barrier properties, the biodegradability is lowered.

TABLE V
T_g Values of Polystyrene–Starch Phthalate Blends

Composition	T_g (K)
Pure PS	368.5
Pure Stph	434.5
20% Stph; 0% C	350.5
20% Stph; 6% C	350.5
40% Stph; 0% C	348.3
40% Stph; 6% C	346.0
50% Stph; 0% C	346.0
50% Stph; 6% C	346.0
60% Stph; 0% C	323.5
60% Stph; 6% C	323.5

For 60% Stph loading, the initial biodegradation rate is lowered for the compatibilized blend but after 75 days, the degradation is accelerated owing to the increased surface area due to the removal of the starch derivative and the pro-oxidant also facilitates the UV degradation of the matrix and in 120 days, the blend showed 85% weight loss.

CONCLUSIONS

Biodegradable blends of PS and esterified starch has been developed using PSGMA for interfacial compatibilization. The mechanical properties such as tensile strength and flexural strength improved on compatibilization although an optimal compatibilizer content of 12% was observed. Water uptake and biodegradability reduced on compatibilization. TGA analysis showed a lower thermal stability than neat PS. DSC thermograms of the blends showed a slight decrease in T_g value from 350.5 K (for 20% stph) to 323.5 K (for 60% stph) with the addition of compatibilizer (Table V).

The authors thank the Department of Science and Technology (DST) for carrying out this work under the Green Chemistry Programme (2007–2010).

References

1. Ramaswamy, M.; Bhattacharya, M. Eur Polym J 1998, 34, 1477.
2. Biresaw, G.; Carriere, J. C. Compos Appl Sci Manuf 2004, 35, 313.
3. Nair, K. C. M.; Diwan, M. S.; Thomas, S. J Appl Polym Sci 1996, 60, 1483.
4. Nair, K. C. M.; Thomas, S.; Groeninckx, G. Compos Sci Technol 2001, 61, 2519.
5. Arvanitoyannis, I.; Psomiadou, E.; Billiaderis, C. G.; Ogawa, H.; Kawasaki, N. J Appl Polym Sci 1997, 33, 227.
6. Arvanitoyannis, I.; Psomiadou, E.; Biliaderis, C. G.; Ogawa, H.; Kawasaki, N.; Nakayama, A. Starch/Starke 1997, 49, 306.
7. Arvanitoyannis, I.; Biliaderis, C. G.; Ogawa, H.; Kawasaki, N. Carbohydr Polym 1998, 36, 89.
8. Arvanitoyannis, I. J Macromol Sci C Polym Rev 1999, 39, 205.
9. Mishra, S.; Naik, B. J. J Polym Plastic Technol Eng 2005, 44, 663.
10. Goad, M. A. H. A. J Appl Polym Sci 2004, 93, 37.
11. Kaewta, K.; Varaporn, T. Carbohydr Polym 2008, 73, 647
12. Lakshmi, N. S.; Cato, L. T. Progr Polym Sci 2007, 32, 762
13. Pathiraja, G.; Roshan, M.; Raju, A. Biotechnol Annu Rev 2006, 12, 301.
14. Ali, S. A.; Fariha, H.; Abdul, H.; Safia, A. Biotechnol Adv 2008, 26, 246.
15. Nassar, A. M.; Abdelwahab, N. A.; Elhalawany, N. R. Carbohydr Polym 2009, 76, 417.
16. Long, Y.; Katherine, D.; Lin, L. Progr Polym Sci 2006, 31, 576
17. Daniela, S.; Maria, J. A. S.; Ines, R. S. Carbohydr Polym 2009, 75, 58.
18. Sagar, A. D.; Merrill, E. W. J Appl Polym Sci 1995, 58, 1647.
19. Willett, L. J. J Appl Polym Sci 1994, 54, 1685.
20. Blisnakov, E. D.; White, C. C.; Shaw, M. T. J Appl Polym Sci 2000, 77, 3220.
21. Zou, Y.; Wang, L.; Zhang, H.; Qian, Z.; Mou, L.; Wang, J.; Liu, X. Polym Degdr Stabil 2004, 83, 87.
22. Zheng, S.; Wang, J.; Guo, Q.; Wei, J.; Li, J. Polymer 1996, 37, 4667.
23. Girija, B. G.; Sailaja, R. R. N. J Appl Polym Sci 2006, 101, 1109.
24. Fras, I.; Boudeulle, M.; Cassagnau, P.; Michel, A. Polymer 1998, 39, 4773.
25. Mano, F. J.; Koiarova, D.; Reis, L. R. J Mater Sci Mater Med 2003, 14, 127.
26. Nassar, A. M.; Abdelwahab, A. N.; Elhalawany, R. N. Carbohydr Polym 2009, 76, 417.
27. Yang, B. Y.; Montgomery, R. Starch/Starke 2008, 60, 146.
28. Tserki, V.; Matzinos, P.; Kokkou, S.; Panayiotou, C. Compos A 2005, 36, 965.
29. Tserki, V.; Matzinos, M.; Panayiotou, C. Compos A 2006, 37, 1231.